



ARCHIVES

of

FOUNDRY ENGINEERING

DOI: 10.1515/afe-2016-0075

Published quarterly as the organ of the Foundry Commission of the Polish Academy of Sciences

DE GRUYTER  
OPEN

ISSN (2299-2944)

Volume 16

Issue 4/2016

11 – 16

# Thermal Stresses in the Wall Connections of Cast Grate Structures

A. Bajwoluk \*, P. Gutowski

Mechanical Engineering Faculty, West Pomeranian University of Technology, Szczecin  
Al. Piastów 19, 70-310 Szczecin, Polska

\*Corresponding author. E-mail address: Artur.Bajwoluk@zut.edu.pl

Received 20.05.2016; accepted in revised form 05.07.2016

## Abstract

The purpose of this study was to establish a relationship between the type of wall connection used in the cast grates, which are part of the equipment operating in furnaces for heat treatment and thermal-chemical treatment, and stresses generated in these grates during the process of rapid cooling. The places where the grate walls are connected to each other are usually characterized by the thickness larger than the remaining parts of walls. Temperature variations in those places are responsible for the formation of hot spots, and in the hot spots temperature changes much more slowly. The type of wall connection shapes the temperature gradient in the joint cross-section, and hence also the value of thermal stresses generated during cooling. In this study, five different designs of the grates were compared; the difference in them was the type of the designed wall connection. The following design variants were adopted in the studies: **X** connections with and without holes, **T** connections with and without technological recesses, and **R** (ring) connection. Numerical analysis was performed to examine how the distribution of temperature changes in the initial phases of the cooling process. The obtained results served next as a tool in studies of the stress distribution in individual structures. The analysis was carried out by FEM in Midas NFX 2014 software. Based on the results obtained, the conclusions were drawn about the impact of different types of wall connections on the formation of thermal stresses in cast grates.

**Keywords:** Application of information technology to the foundry industry, Cast grates, Thermal stresses

## 1. Introduction

Accessories of furnaces for heat treatment and thermal-chemical treatment are exposed to the impact of many unfavourable factors. These include, among others, high temperature, rapid changes of temperature (especially during cooling of the charge) and the effect of strongly carburizing atmosphere. Cast grates, which are part of furnace accessories, are additionally loaded with charge, which is resting on them during the heat treatment.

All these factors shorten the life of the grates. The most frequent direct causes of withdrawal from further use are emerging cracks and excessively large changes of external

dimensions caused by structure deformations cumulating in subsequent cycles [1-3]. For the crack formation and piling up of deformations are responsible stresses that arise in castings subjected to rapidly changing temperatures. Understanding the mechanism of their formation during operating cycles can therefore have a significant contribution to the improvement of equipment reliability.

Damages to the grates operating under drastic temperature changes are usually associated with the presence of stresses due to differences in the thermal expansion of the cast steel components and stresses caused by temperature gradients in the cross-section of the cooled components [1, 3-5]. Grates are typically cast from the stable austenitic steels with high nickel content, and therefore in the discussion of the causes of damage, stresses due to phase

transformations can be neglected [6].

The study described in [7] discusses, among others, the relationship that is believed to exist between the type of wall connection used in the cast grates and temperature gradient in the wall cross-section. **T**-connections with and without technological recesses and **X** connections were examined. Tests were carried out on individual elements of the grates, first, to make similar analysis for more complex components of the grates, next, and end in the analysis of the whole grate structure composed of the individual elements examined at the beginning. Consequently, analysis covered the heat flow in the five proposed structures of the cast grates, differing from each other in the type of the designed wall connection. Then, the examined structures were compared in terms of the thermal stresses formed in them. The article presents the results of the conducted analysis.

## 2. Models of test grates

Studies covered the simulation and analysis of five grate structures differing in the type of the designed wall connection. The base structure was the grate in which the walls were joined by the **X** type connection. In comparative structures, this connection was replaced with the **T**-type connection and with the connection modified to **X<sub>m</sub>** provided with a through-hole as a means to reduce the hot spots forming there. Additionally, studies also included some selected designs using **T**-type connections modified with technological recesses (**T<sub>m</sub>**) and a ring connection (**R**). For analysis, the following geometric parameters of the grates were adopted: wall thickness – 8 mm, fillet radius – 6 mm, height of the grate – 50 mm and outer dimensions, i.e. width and depth, 358 × 358 mm, respectively. Considering the fact that the test structures were symmetrical in relation to the three main planes ( $Oxy$ ,  $Oxz$ ,  $Oyz$ ), calculations were performed on models representing 1/8 of the entire structure of the grate (reduction by half of each of the main planes as shown in Fig. 1), thus shortening considerably the time required for calculations. Models used for the simulation and analysis (Fig. 2) were designed in SolidWorks, while calculations were performed in Midas NFX 2014 software.

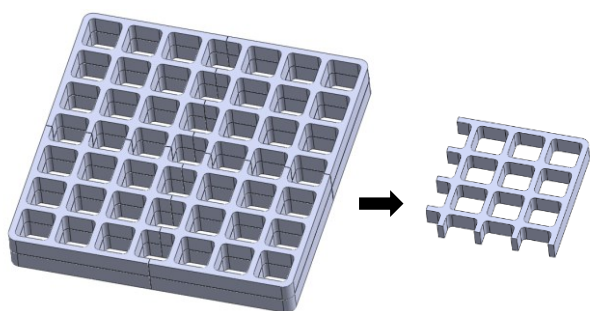


Fig. 1. Calculation area reduced to 1/8 of the original area of the grate

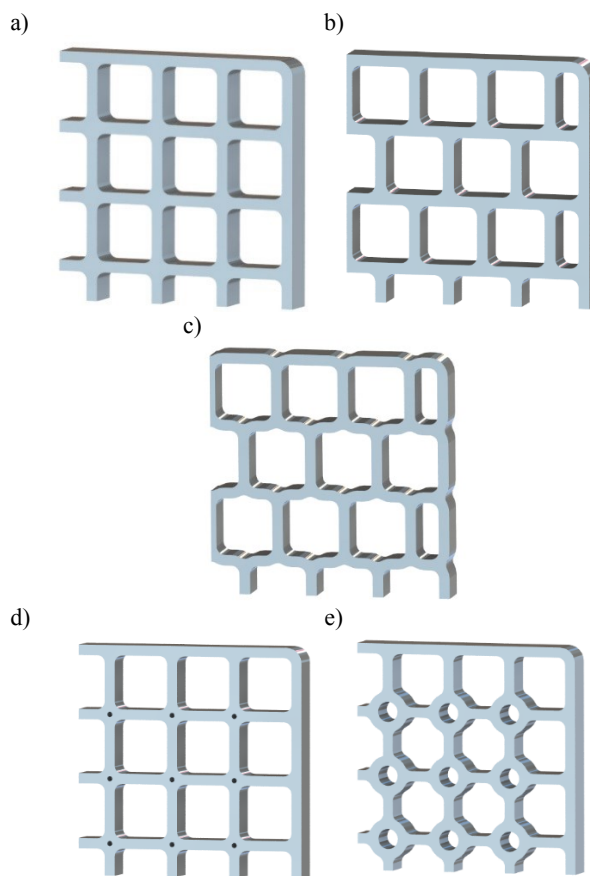


Fig. 2. Models of grate design with different types of connections adopted in the analysis: a) **X**, b) **T**, c) **T<sub>m</sub>**, d) **X<sub>m</sub>**, e) **R**

## 3. Heat flow analysis

The first stage of the studies was devoted to a numerical analysis of the grate cooling process. The temperature of  $T_0 = 900^\circ\text{C}$  was adopted as a starting point in calculations. Cooling was done in oil at a temperature of  $T_k = 40^\circ\text{C}$ . Heat transfer in the grate-environment system takes place through convection, while in the interior of the cast grate, it is the conductivity that controls this process. In this study, the curve of the heat transfer coefficient (Fig. 3) consistent with the curve proposed in [8] has been used. Thermal parameters of the cast material (steel) were chosen in accordance with EN 10295: 2002 [9], adopting the following values: the specific heat of cast steel  $C_s = 500 \text{ J}/(\text{kg} \cdot \text{K})$  and thermal conductivity  $\lambda$  derived from the curve based on the data given in Table 1 of the aforementioned standard. The computational step of analysis was  $\Delta t = 0.33 \text{ s}$ .

Table 1.  
The coefficient of thermal conduction  $\lambda$  of cast steel 1.4849 [9]

Temperature $T$ , $^\circ\text{C}$	20	100	800	1000
Coefficient $\lambda$ , $\text{W}/(\text{m} \cdot \text{K})$	12	12,3	23,3	26,5

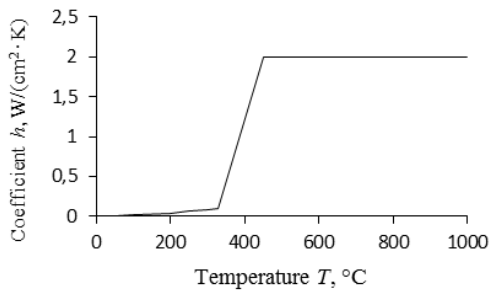
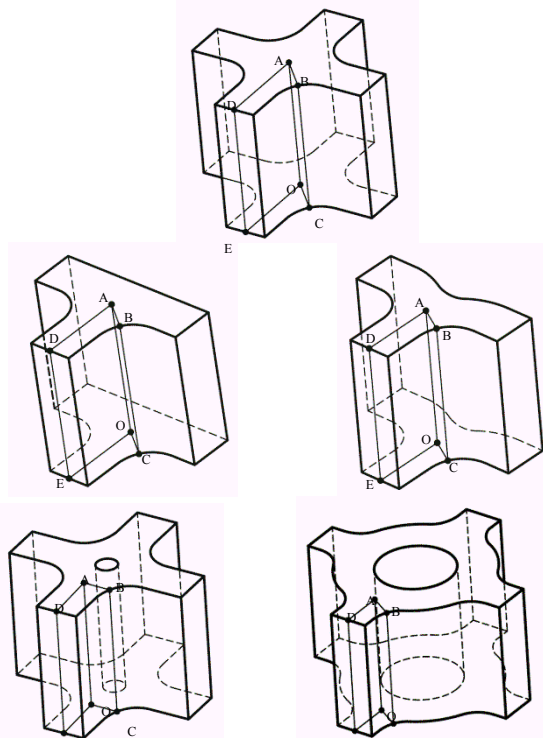


Fig. 3. Coefficient of heat transfer during cooling

The structure of the grate with areas of the varying thickness is responsible for the different cooling rates, resulting in the formation of temperature gradients not only between the centre and the surface of cast wall, but also between the centre of connection and the centre of connected ribs.

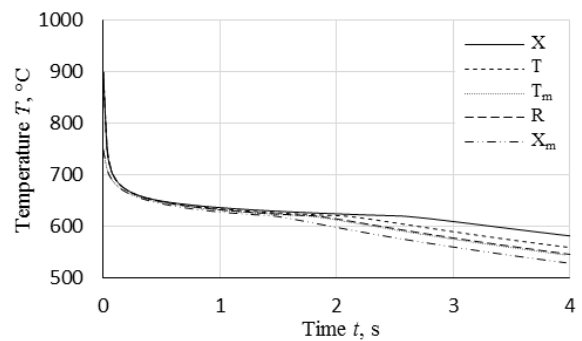
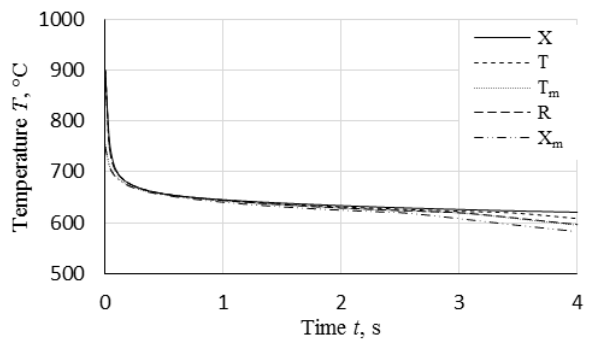
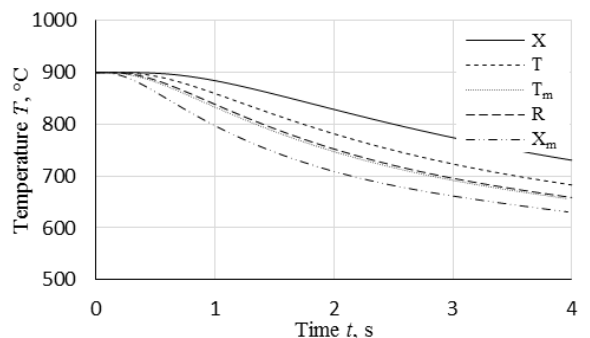
Figure 4 shows different types of wall connections used in the examined models of the grate structure. Two characteristic planes, i.e.  $OADE$  and  $OABC$ , are marked on them.

Fig. 4. The orientation of the surfaces  $OABC$  and  $OADE$  in each of the examined connections

The former is the plane of symmetry between the wall and the connection, the latter is the plane where the distance between the centre of the connection and its surface is measured. In these planes, the important points are marked for further evaluation of the thermal behaviour and strength. Point  $O$  is the centre of the connection of two walls (the centre of hot spot). Points  $A$  and  $C$  are lying on the surface - the first one ( $A$ ) above the point  $O$  and

the second one ( $C$ ) close to this point. The centre of the grate wall with a regular thickness is designated as point  $E$ .

In all the designs tested, the temperature inside the wall (point  $E$ ) has been changing in a similar way. At other specified points, temperature changes in time were plotted in the form of graphs shown in Figures 5 - 7. It is clear that, irrespective of the design, in the first phase of cooling (until about 1.5 sec), the temperature at points  $A$  and  $C$  is almost identical. The deviations that appear in further stages of the cooling process are due to the formation of hot spots, which act as heat accumulators. The different impact of hot spots present in each of the examined solutions is best seen on the graph in Figure 7, which shows temperature changes at point  $O$ .

Fig. 5. Temperature changes on the surface of the grate – point  $A$ Fig. 6. Temperature changes on the surface of the grate – point  $C$ Fig. 7. Temperature changes in the interior of the grate – point  $O$ 

The point is in the centre of the wall connection and thus represents the place with the highest temperature. It is rather

obvious that in the case of this particular place, the type of connection will have a significant impact on the rate of temperature changes. In structures with the connections characterized by a large centre-to-surface distance, the drop of temperature in the hot spot shows a distinct delay.

The factor that controls the occurrence of thermal stresses in a given direction in the cooled or heated component is mainly the temperature gradient acting in this direction. Simulation and respective calculations of the temperature distribution changing in time were performed for all the examined types of connections. Sample results of calculations of the difference in temperature between point *O* and points *A*, *C* and *E* for the **X** type connection are presented in Figure 8. In addition to this drawing, a graph has been provided showing time-related variations in the temperature difference between point *O* and point *B*, which is the point in the connection characterized by the highest cooling rate.

It is evident that temperature differences between the centre of the connection and points lying on the surface (*A*, *B*, *C*) are characterized by the highest values at the beginning of the cooling process. As regards the temperature difference between points *O* and *E*, the value is low at the beginning of the process. It raises with time and is close to maximum for a time much longer than the difference between the interior of the connection and its surface.

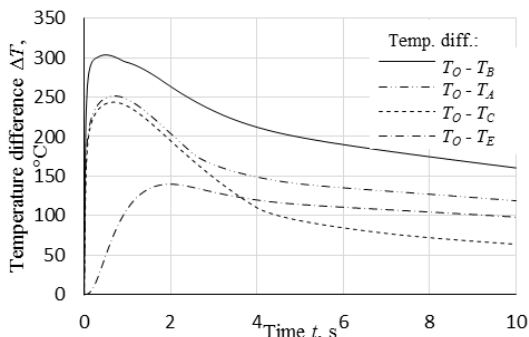


Fig. 8. Temperature differences changing during cooling of the grate in the **X** connection centre (*O*), in the wall centre (*E*) and in the wall surface (*A*, *B*, *C*)

The data on temperature differences at various points in the grate structure are insufficient to provide comprehensive information about places where changes in the temperature are most rapid and temperature gradient assumes the highest value. Therefore, Figures 9 and 10 show temperature distribution in the directions *OA* and *OC* (the smallest distance between the central point of the connection and its surface in the directions both vertical and horizontal) and in the direction *OE* after 0.5 and 1.5 seconds of the cooling process, respectively. It is evident that in the directions from the centre of the connection towards its surface (the directions *OA* and *OC*), the greatest temperature changes occur at the surface, and there the highest stresses are to be expected. In the direction between points *O* and *E*, the greatest change of temperature occurs in the vicinity of point *O*. This change, as shown on the graph in Figure 8, is visible only at a more advanced stage of cooling.

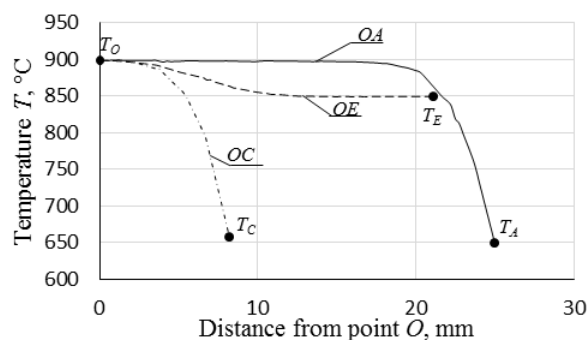


Fig. 9. Temperature distribution in the **X**-type connection in the directions *OA*, *OC* and *OE* after 0.5s of the cooling process

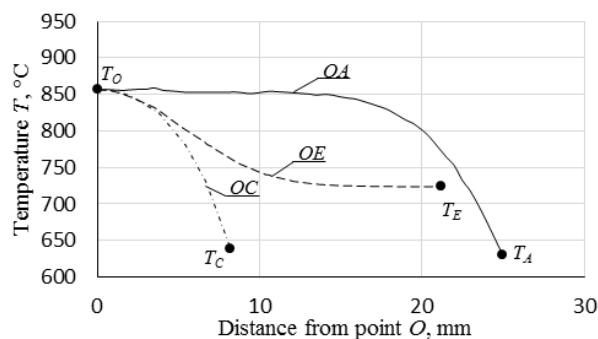


Fig. 10. Temperature distribution in the **X**-type connection in the directions *OA*, *OC* and *OE* after 1.5s of the cooling process

Depending on the type of connection used in cast grates, the resulting differences in temperature tend to assume different values. Table 2 lists maximum temperature differences noticed in the examined structures of the grates. It is evident that the base design using a plain **X** connection is characterized by the greatest differences of temperature. In the case of other connections, the resulting gradients are lower, which is associated with the less pronounced differences in the thickness of the single walls and several walls joined together.

Analysis of the results compared in Table 2 shows that different types of connections vary in their effectiveness of reducing to minimum the maximum temperature gradients, depending on whether the difference between the centre of the connection and its surface is considered (the directions *OA* and *OC*), or whether it is the difference between the centre of the connection and the centre of the wall (the direction *OE*). In the first case, the effect is much weaker and difficult to notice. Variations in the calculated maximum temperature difference ( $\Delta T_{OA}$  and  $\Delta T_{OC}$ ) between the design using **X**-type connection and the design with other types of connections are less than 9%.

In the second case, the impact of the type of connection on the temperature gradient during cooling is much more prominent. The best result in the group of the tested connections (the smallest temperature difference between the centre of the connection and the centre of the wall) was obtained for the modified **X<sub>m</sub>** connection with a hole designed to reduce the effect of hot spots. In this case, the temperature difference between the centre of the connection and the centre of the wall was 25.8°C (which is equal to 18.4% of the maximum temperature difference obtained for the

base design with X-type connection).

Table 2.

Maximum temperature differences in various directions

Type of connection	$(\Delta T_{OE})_{\max}$ [°C]	$(\Delta T_{OC})_{\max}$ [°C]	$(\Delta T_{OA})_{\max}$ [°C]
<b>X</b>	139.9	243.8	251.7
<b>X<sub>m</sub></b>	25.8 (39.7)	222.9	230.3
<b>R</b>	65.6	230.4	238.6
<b>T</b>	88.4	236.0	243.9
<b>T<sub>m</sub></b>	64.0	230.1	238.1

It should be noted, however, that in this design the thinnest place is not the grate wall, but the cross-section lying between the hole and the fillet of the wall connection. The temperature difference between the centre of the connection and the centre of this cross-section is 39.7°C (28.4%). An alternative to this connection may be a ring-type connection. In this case, the temperature difference between the centre of the connection and the centre of the wall is 65.6°C (46.9%). A similar result was obtained for the modified **T<sub>m</sub>** connection with technological recesses. This result was by 27.6% better than the result obtained for the plain **T** connection.

Heat transfer analysis showed changes of temperature distribution in the walls of the grates losing heat and related these changes to the type of connection designed for the grate walls, thus making a first comparison of the adopted design solutions.

## 4. Thermal stress analysis

The results of studies of the heat transfer in the cooled structures of cast grates were used as input data for the analysis of stresses generated during this process. In these calculations, each node of the finite element mesh was loaded with the preset change of temperature from 900°C to a temperature which, within the accepted time limit of the cooling process, was calculated for the mesh nodes in studies of the changes in temperature distribution.

Since studies were carried out on models representing 1/8 of the grate structure, nodes lying on the three main planes ( $Oxy$ ,  $Oxz$ ,  $Oyz$ ) were restrained in directions perpendicular to these planes. Nodes situated on the main axes were deprived of freedom in two directions.

In the analysis, the cast steel of the following mechanical properties was used: Young's modulus  $E = 1.73 \cdot 10^5$  N/mm<sup>2</sup>, yield strength  $R_e = 208$  N/mm<sup>2</sup>, the strain-hardening modulus  $E_e = 4.09 \cdot 10^3$  N/mm<sup>2</sup>, the thermal expansion coefficient  $\alpha = 1.77 \cdot 10^{-5}$ , Poisson's ratio  $\nu = 0.253$  [4].

The results of calculations are presented in the form of charts in Figures 11-14. They show the distribution of reduced stresses (calculated in accordance with the Huber-Mises hypothesis) in the directions designated as *OE* (Figs. 11 and 13) and *OC* (Figs. 12 and 14) with the thermal load applied on mesh nodes by the temperature calculated after 0.5 s (Figs. 11 and 12) and 1.5 s (Figs. 13 and 14) of the cooling process. However, for the correct interpretation of results, it has to be remembered that different connections have different minimum distance between the centre (*O*) and the surface (*C*). To make the comparison easier, the

graphs shown in Figures 12 and 14 have the values on the abscissa which express not the real distance of a given point from the centre of the connection (point *O*) but a normalized distance, which is the ratio of the actual distance from point *O* to the distance *OC*.

Careful analysis of charts with the plotted values of stress reduced after 0.5s shows that the values and the distributions of stresses are very similar in all the tested connections. This is consistent with the results of the heat flow analysis, wherefrom it follows that after this time the impact of the connection as a heat accumulator is still so weak that the type of design used in each case has only a minor effect on the values of the resulting thermal stresses.

The distribution of stresses after 1.5 s of the cooling process shows a much more prominent effect of the different types of connections. Stress generated in the structure with the **X**-type connection, where the greatest differences in temperature have been recorded, now reaches the highest value and in a large area exceeds the allowable yield strength limit. The allowable yield strength limit has also been exceeded, though to a smaller extent, in the case of the **T**-type connection. Slightly lower values of reduced stress were recorded for the **T<sub>m</sub>** connection and **R** connection. The lowest values were obtained in the **X<sub>m</sub>** connection with a small hole. These results are consistent with the maximum temperature differences reported to take place between the centre of the connection and the centre of the wall, as shown in Table 2.

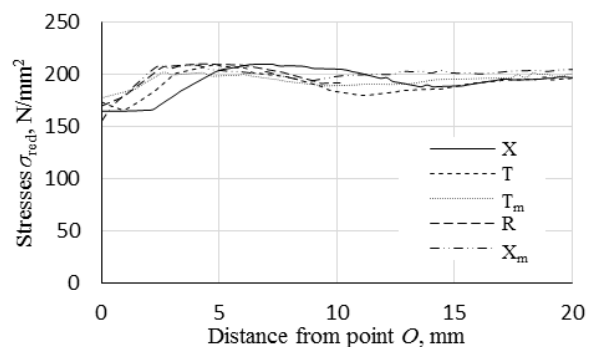


Fig. 11. Distribution of reduced stresses in the direction OE after 0.5s

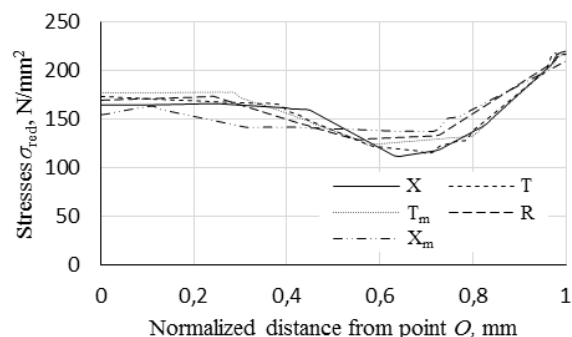


Fig. 12. Distribution of reduced stresses in the direction OC after 0.5s

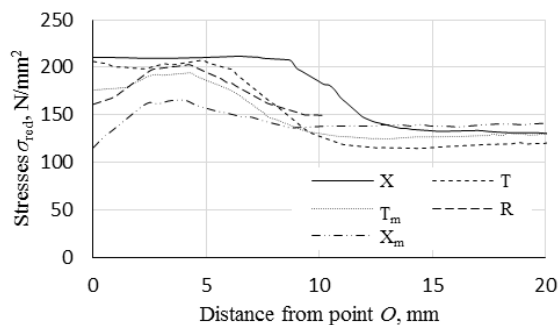


Fig. 13. Distribution of reduced stresses in the direction OE after 1.5s

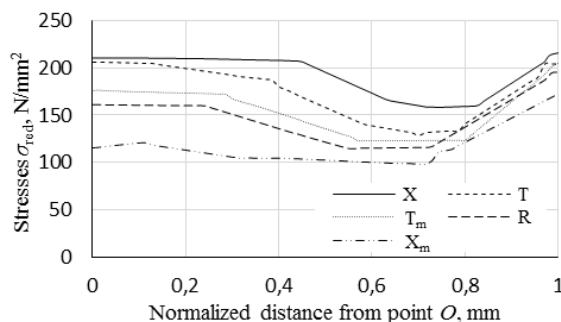


Fig. 14. Distribution of reduced stresses in the direction OC after 1.5s

## 5. Summary

Studies covered the simulations of changes in the temperature distribution during cooling of cast grates and in the thermal stresses generated at the beginning phases of this process. The obtained quantitative results are consistent with the theoretical knowledge and with the results of calculations carried out for individual elements. In the heavy connections with a large volume, temperature changes are proceeding much more slowly than in the wall joints. The result is the formation of large temperature gradients and high stresses arising in the structure being cooled.

The obtained results indicate that the effect of the type of connection on the generated stresses is of minor importance only at the very beginning of the cooling process. This is due to the fact that in the early phase of the process both wall centre and the centre of connection have similar temperature (close to the initial one) and temperature gradient is formed only between the core of the material and its surface (the greatest changes in temperature occur at the surface).

Slower changes in temperature, characteristic of the wall connections, have more serious effect on the formation of thermal stresses in the subsequent phases of cooling, when the hot spots start acting as heat accumulators. After this time, the worst results among all the tested design solutions has yielded the base design with the plain X-type connection and the design with the plain T-connection, where stresses due to the temperature gradient assumed the highest values.

Optimal in respect of the thermal stress reduction to a minimal level has turned out to be the  $X_m$  design with a small hole. However, from a technical point of view, this is the design most difficult to perform. Hence, the preferred solutions used in the actual design of cast grates are ring connections **R** and **T<sub>m</sub>** connections with technological recesses. The fact that the effect of the type of connection shows up not in the first cooling phase, which takes the most rapid course and generates the greatest temperature differences, but in the subsequent phases of the process suggests that thermal stresses associated with the formation of hot spots cause plastic deformation of the grates, that is, their permanent deformation rather than the rapid cracking.

Analysis of the hot spots formed in cast grates should be made as a first step in the assessment of the technological applicability of various design solutions used in the construction of the cast grates. Numerical calculations are a quick and relatively cheap tool helping to detect the sites of the slowest temperature changes and, if permitted by reasons of a technological nature, to introduce some modifications to the structure and remove these sites. The next step in the analysis of the grate design should be the stress-strain analysis, taking into account the impact of charge loading the grate.

## References

- [1] Piekarski, B. (2012). *Creep-resistant castings used in heat treatment furnaces*. Szczecin: College Publisher Zachodniopomorskiego Uniwersytetu Technologicznego, (in Polish).
- [2] Piekarski, B. & Drotlew, A. (2008). Designing of castings working in conditions of temperature cyclic changes. *Archives of Mechanical Technology and Automation*. 28(3), 95-102. (in Polish).
- [3] Drotlew, A. & Piekarski, B. (2001). Creep resistant casting of grates – constructional and technological notice. *Archives of Foundry*. 1(1), 446-453. (in Polish).
- [4] Gutowski, P. (1989). *Research the causes of cracking in pallets operating in furnaces for the carburising treatment*. Doctoral dissertation, Technical University of Szczecin, Szczecin. (in Polish).
- [5] Gutowski, P. & Tuleja, J. (2006). The effort analysis of fracture propagation in stable austenitic casting alloy under rapid changes of temperature. *Archives of Mechanical Technology and Automation*. 25(1), 25-37 (in Polish).
- [6] Kubicki, J., Christodulu, P. (1983) The stability of chromium-nickel steel under condition of carburising treatment and thermal shock. In IX Scientific Symposium on the Occasion of Caster, part 1. 93-99. Kraków: AGH. (in Polish).
- [7] Bajwoluk, A. & Gutowski, P. (2015). The effect of pallet component geometry on temperature gradient during cooling. *Archive of Foundry Engineering*. 15(1), 5-8. DOI: 10.1515/afe-2015-0001.
- [8] Bajwoluk, A. & Gutowski, P. (2014). Analysis of thermal stresses in components of pallets operating in furnaces for the carburising treatment. *Archive of Foundry Engineering*. 14(spec.1), 175-180.
- [9] Standard EN 10295:2002. Heat resistant steel castings.